# Off-center lithium in the fluoroperovskite $KZnF_3$

J. Toulouse and X. Q. Wang
*Physics Department, Lehigh University, Bethlehem, Pennsylvania 18015*

M. Rousseau
*Laboratoire de Physique de l'Etat Condensé, Faculté des Sciences, 72017 Le Mans CEDEX, France*
(Received 16 July 1990; revised manuscript received 31 May 1991)

In studying the effect of point defects on structural phase transitions in fluoroperovskites, we have characterized the Li defect in $KZnF_3$. The dielectric-loss measurements on $KZnF_3$:Li have revealed that the lithium defect possesses an electric dipole moment and therefore sits in an off-center position approximately 0.15 Å from a normal K site. Complementary ultrasonic measurements of the sound velocity indicate that Li constitutes a $\langle 100 \rangle$ orthorhombic defect. The $\delta v/v$ results indicate that, similar to the KBr-KCN system, the strain ellipsoid is not an ellipsoid of revolution. The shape factors of the ellipsoid are found to be $\lambda_a - \lambda_b \sim 0.013$ and $\lambda_b - \lambda_c \sim 0.006$. This translates into two distinct relaxation processes at high and low temperatures, respectively, primarily associated with the reorientation of the major and minor axes of the ellipsoid. The dielectric-loss peak is then associated with the relaxation of the lithium defect between the three cube axes, i.e., the major-axis reorientation. The above interpretation is consistent with the large anharmonicity and anisotropy that have been found in the motion of the fluorine ions in $KZnF_3$ and other related fluoroperovskites exhibiting a soft mode.

## I. INTRODUCTION

Several theoretical studies in the last fifteen years have addressed the question of the role of point defects at or near structural phase transitions. It has become evident that this role depends crucially upon the nature of the defect, whether symmetry breaking or non-symmetry-breaking, mobile or frozen.[1] Experimentally, it has been suggested that point defects may be responsible for central peaks observed in neutron or light scattering.[2] In order to interpret the data and to construct physical models it is however necessary to first obtain a precise model of the defect involved. In the present study, we have attempted to determine the nature of the defect formed by a lithium impurity atom in fluoroperovskites. In a later paper we will examine the effect of the defect on the phase transition. The two particular systems chosen are $KZnF_3$ and $KMnF_3$. Both are structurally identical and they also have comparable lattice parameters, 4.053 Å and 4.190 Å, respectively.[3] With regards to their lattice dynamics, both systems exhibit a soft zone boundary phonon mode. In $KMnF_3$ the softening of this mode leads to a ferroelastic transition at $\sim 186$ K. In $KZnF_3$, however, the soft mode lies in a higher frequency range so that its frequency remains finite down to absolute zero and no transition takes place.[3]

This pair of systems constitutes a very convenient one, in which $KZnF_3$ can be primarily used to identify the defect and the possible interaction with the soft mode, and $KMnF_3$ can be used to study the effect of this defect on the phase transition.

The particular impurity chosen in the present study is lithium. This choice was directed by the fact that Li in many systems is known to form an interstitial defect, which is therefore symmetry breaking and can thus, in principle, be detected dielectrically and elastically. In Sec. II we review the theory of dielectric loss and ultrasonic dispersion due to point defects in solids. The experimental conditions are described in Sec. III. In Sec. IV we present the results and in Sec. V, we discuss the defect model mandated by these results.

## II. THEORY

### Dielectric loss (Ref. 4)

The dielectric response of a solid to a small ac field can usually be expressed in terms of a complex dielectric constant:

$$\epsilon^* = \epsilon' - i\epsilon'' = \epsilon e^{i\delta} , \tag{1}$$

The dielectric loss is then written as the tangent of the phase angle, $\delta$, between the applied field and the resulting polarization where

$$\tan\delta = \epsilon''/\epsilon' . \tag{2}$$

Using Debye theory, the loss due to the relaxation of point defects is written as

$$\tan\delta = \frac{\Delta\epsilon}{\epsilon(0)} \frac{\omega\tau}{1+\omega^2\tau^2} , \tag{3}$$

where $\tau$ is the relaxation time in which the electric dipoles reach their new equilibrium position in the presence of an applied field, $\Delta\epsilon = \epsilon(0) - \epsilon(\infty)$ and $\epsilon' \simeq \epsilon(0)$. Using a simple orientational polarizability model for noninteracting dipoles in three dimensions we find

$$\Delta\epsilon = \frac{Np^2}{3kT} \tag{4}$$

 

in which $N$ is the concentration of dipoles per unit volume and $p$ is the dipole moment and where we assume that the local field is equal to the applied field. For a given radial frequency of the applied field, the maximum loss is obtained when the condition $\omega\tau=1$ is satisfied. The peak height is then seen to be

$$\tan\delta_{\max}=\frac{\Delta\epsilon}{2\epsilon(0)} . \tag{5}$$

### Ultrasonic dispersion (Ref. 5)

All permanent electrical dipoles associated with point defects in solids must also possess an elastic dipole, however small it may be. The elastic dipole movement for a defect in an orientation $p$ is written as

$$\lambda_{ij}^{p}=\partial\epsilon_{ij}/\partial c^{p} , \tag{6}$$

where $\lambda_{ij}$ is the $(ij)$ component of the strain and $c^p$ is the molar concentration of defects in orientation $p$. By analogy with the dielectric case, and at high enough temperature ($\omega\tau\ll 1$), we can expect that the elastic dipole will reorient in the strain field of the sound wave, thereby decreasing the velocity of the wave. Using simple Maxwell-Boltzmann statistics, the velocity change, $\delta v/v$, due to the presence of the defects can be calculated and expressed as

$$\frac{\delta v}{v}=\frac{1}{2}C\frac{c_0 v_0}{n_t kT}\left[\sum_p(\lambda^p)^2-\frac{1}{n_t}\left[\sum_p\lambda^p\right]^2\right] , \tag{7}$$

where $C$ is the appropriate elastic stiffness constant, $c_0$ the average defect concentration, $v_0\equiv V/N_A$ with $V$ the molar volume, $N_A$, Avogadro's number, and $n_t$ the number of elastically distinguishable orientations. The factor between large square brackets is expressed in terms of the principal values of the $\lambda$ tensor. According to group theory, this factor is nonzero only if there exists a symmetry coordinate of the elastic dipole belonging to the same irreducible representation as the strain field of the sound wave. This condition gives rise to selection rules that are summarized in Table I. In this table, the entries represent the number of independent reorientation processes that can give rise to the relaxation of a particular elastic constant. A $\langle 100\rangle$ orthorhombic defect, for instance, can couple to an $E$-type sound wave giving rise to two possible reorientation processes of the defect. The same defect cannot, however, couple to a $T$-type sound wave. Each process is characterized by a distinct relaxation time $\tau$. In the case cited above of an orthorhombic defect, the two relaxation times can be expressed in terms of the specific reorientation frequencies involved as[6]

$$\tau^{-1}=(\nu_{12}+3\nu_{13}+\nu_{14}+\nu_{16}) \pm\frac{1}{\sqrt{2}}[(\nu_{12}-\nu_{14})^2+(\nu_{14}-\nu_{16})^2+(\nu_{12}-\nu_{16})^2]^{1/2} \tag{8}$$

in which $\nu_{ij}$ designate the jump frequency between any two of the six possible defect configurations. These configurations are easy to visualize if we note that a $\langle 100\rangle$ orthorhombic defect can be viewed basically as a tetragonal defect for which the distortion is not an ellipsoid of revolution but possesses two distinct minor axes. Therefore, for each of the three cubic axes, there are two possible orientations of the minor axes of the ellipsoid.

We can also predict the relative magnitudes of $\delta v/v$ for different waves. In particular we can write $C_{11}$ (stiffness constant for longitudinal [100] waves) in terms of symmetry constants

$$C_{11}=\tfrac{1}{3}[(C_{11}+2C_{12})+2(C_{11}-C_{12})]$$

in which $(C_{11}+2C_{12})/3$ is the bulk modulus. Because the latter cannot give rise to a relaxation under a uniaxial strain we can write

$$\frac{\delta C_{11}}{C_{11}}=\frac{2}{3}\frac{(C_{11}-C_{12})}{C_{11}}\frac{\delta(C_{11}-C_{12})}{C_{11}-C_{12}} . \tag{9}$$

Using Eqs. (7) and (9), we can then obtain an expression for $\delta v/v$ ([100] longitudinal):

$$\left.\frac{\delta v}{v}\right|[100]_{100}=-\frac{1}{9}\frac{(C_{11}-C_{12})^2}{C_{11}}\frac{c_0 v_0}{kT}(\lambda_1-\lambda_2)^2 \tag{10}$$

in which $\lambda_1$ and $\lambda_2$ represent two of the principal values of the elastic dipole tensor. The fractional change in the shear constant $(C_{11}-C_{12})$ can also be obtained directly from a [110] transverse wave.

## III. EXPERIMENTAL

The crystals used in this study were grown in LeMans (France), starting from optical grade $ZnF_2$ and $MnF_2$ powders and using the Bridgman technique. Lithium was introduced by the addition of 99.99K pure LiF to the melt. Three $KZnF_3$ crystals were grown for this study, one pure and two doped with nominally 1% and 2% Li. The actual concentrations were estimated by flame absorption spectroscopy and found to be 630 and 1900 ppm, respectively. However, as will be shown later, a relatively steep concentration gradient was found to exist in these crystals so that these concentrations are only approximate. In the remainder of this paper we shall use the nominal concentration to designate the doped crystals. The crystals were oriented by x-ray diffraction which also revealed the presence of residual internal strains with a preferred orientation. The dielectric samples were cleaved in the form of thin plates ($\sim 1\times 1\times 0.1$ $cm^3$) and the ultrasonic samples were approximately cubic ($\sim 1\times 1\times 1$ $cm^3$), also obtained by cleavage from the boules. The 1% dielectric sample was cut just above the corresponding ultrasonic sample.

For the measurements, the samples were placed in appropriate holders which were then screwed into the cold finger of a Janis cryostat. The temperature was monitored with two silicon diodes and regulated with a DC 91 Lake Shore controller. The dielectric measurements were performed with a General Radio 1615A capacitance bridge at frequencies between 200 Hz and 10 kHz. The ultrasonic set up and sample holder have been described elsewhere;[7] the RF frequency used was 45 MHz.

TABLE I. Selection rules for anelastic relaxation of defects. The numbers corresponding to each defect symmetry correspond to the number of distinct relaxation processes allowed by symmetry.

| Propagation direction | Polarization direction | Velocity | Strain symmetry | Defect Symmetry Tetragonal | Trigonal | Orthorhombic ⟨100⟩ | Orthorhombic ⟨110⟩ | Monoclinic ⟨100⟩ | Monoclinic ⟨110⟩ | Triclinic |
|---|---|---|---|---|---|---|---|---|---|---|
| [100] | [100] | $\sqrt{C_{11}/\rho}$ | $A_{1g}$, $E_g$ | 1 | 0 | 2 | 1 | 2 | 1 | 2 |
| [100] | [010] | $\sqrt{C_{44}/\rho}$ | $T_{2g}$ | 0 | 1 | 0 | 1 | 1 | 2 | 3 |

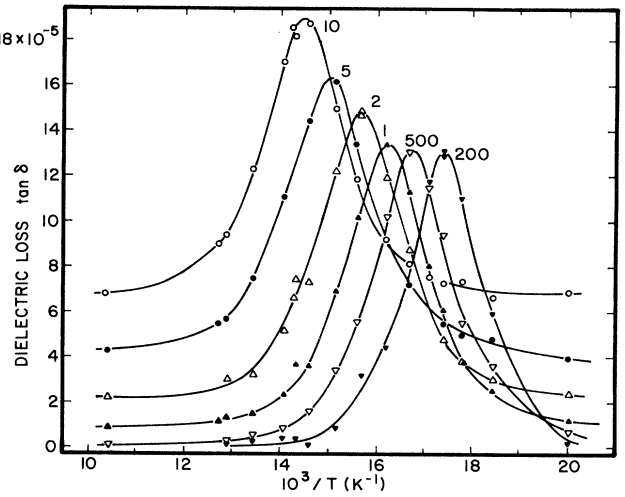


FIG. 1. Dielectric loss, tan δ, vs. temperature for different frequencies in Hertz. ($KZnF_3$:Li, approximate concentration 300±50 ppm).

## IV. RESULTS—DIELECTRIC LOSS IN $KZnF_3$

Dielectric loss was measured on several $KZnF_3$ samples. No loss peak was observed in the pure sample. The results obtained on the 1% sample are presented in Fig. 1 for six different frequencies. The presence of lithium results in a well defined loss peak. Very similar results were obtained on a second 1% sample. The 2% sample also showed a peak, that was however lower in height and broader in width, probably due to crystalline defects or defect interactions. Because of the excellent quality of the data obtained on the 1% sample, they are the ones used in the following analysis. The dielectric-loss results have been analyzed in two different ways. First, the loss peaks have been fitted to a single Debye relaxation peak. An example of the goodness of the fit is shown in Fig. 2 for 10 kHz. The activation energies obtained from those fits vary between 0.112 and 0.124 eV with a mean of 0.118 eV. The prefactor correspondingly varies between $1.2\times10^{-13}$ and $1.2\times10^{-14}$ s with a mean of $5.7\times10^{-14}$ s. Second, according to the condition for maximum loss, $\omega\tau=1$, we have used the position of the peak at each frequency to determine the relaxation time $\tau(T)$. In Fig. 3, we have plotted $\tau(T)$ on a semilog scale for the two 1% samples measured. The relaxation time clearly obeys an Arrhenius-type law which can be written as

$$\tau=2.6\times10^{-14}\exp[(0.121\text{eV})/\text{kT}]\ ,$$

where the prefactor is expressed in units of seconds and the activation enthalpy in eV, both values obtained from a linear regression fit. A comparison of the enthalpy values, respectively, obtained by the two methods above reveals only a small difference, which means that the observed loss peak is very close to being a perfect Debye peak. We can calculate the relative broadening of the observed peak, using the second value, $H=0.121$ eV, which

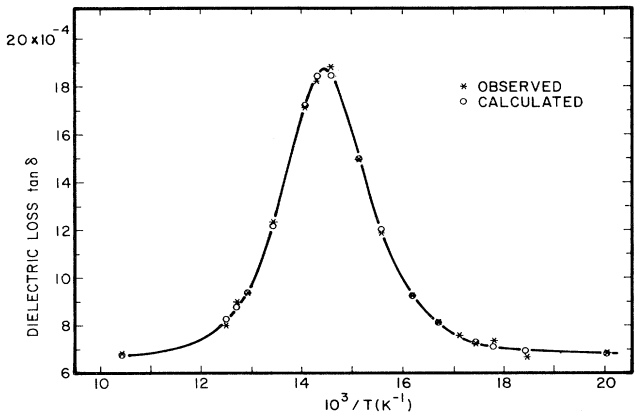


FIG. 2. Dielectric loss, tan δ, vs. temperature for a 10-kHz applied field. The solid line corresponds to a single Debye relaxation model with parameter values as indicated in the text.

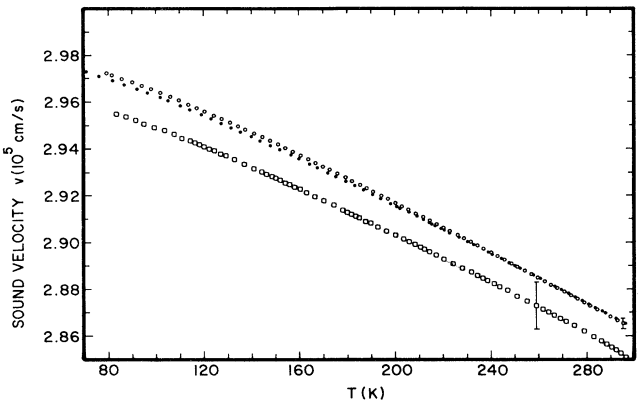


FIG. 4. Sound velocity vs. temperature in $KZnF_3$ pure ○; 1057 ppm Li, ●; 1900 ppm Li, □. The error bars only reflect the experimental uncertainty on the absolute velocities at room temperature, and do not affect the relative values.

does not *a priori* assume a Debye relaxation. The theoretical width of the corresponding Debye peak is then predicted to be[5]

$$\Delta(1/T)=2.635k/H=1.88\times10^{-3}\ \mathrm{K}^{-1}\ ,$$

Comparing with the experimental width (Figs. 1 and 2) we conclude that the observed peaks are only about 2% wider than the theoretical Debye peaks; it is thus clear that the relaxation observed can be attributed to a simple isolated Li defect which possesses an electric dipole. The small value of the enthalpy suggests that the Li impurities form an *off-center defect* in $KZnF^3$. Based on valence consideration, the lithium off center most likely substitutes for potassium. Off-center Li defects are already known in other ionic crystals, e.g., KCl (Ref. 8) and $KTaO_3$ (Ref. 9).

## V. ULTRASONIC RESULTS IN $KZnF_3$

Because the dielectric tensor of a cubic crystal consists of a single component,[10] it is not possible to determine the orientation of the off-center Li defect simply from dielectric measurements. In order to complement the dielectric loss data obtained in $KZnF_3$, we have therefore made measurements of the velocity of ultrasonic waves. The propagation directions and polarizations of the waves used are given in Table I, along with the expressions for their respective velocities given in terms of elastic constants. As an example, the velocity results corresponding to the $C_{11}$ constant obtained from a [100] propagating wave are shown in Fig. 4 for the pure and two Li doped crystals. For the present purpose however, the most interesting presentation of the results is given in Fig. 5 as $\delta v/v$ vs. $1/T$. Here $\delta v$ represents the difference

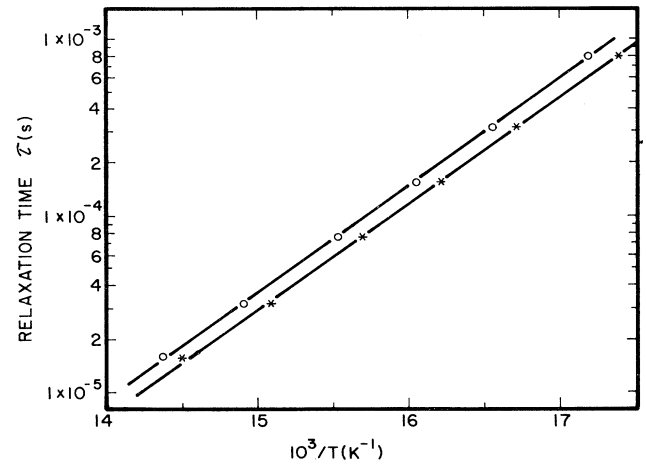


FIG. 3. $\tau(T)$ vs. $10^3/T$. A semilogarithmic plot corresponding to the data shown in Figs. 1 and 2.

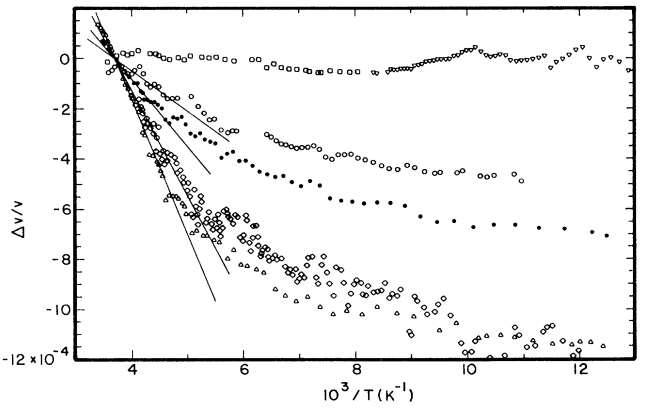


FIG. 5. $\delta v/v$ vs. $10^3/T$ in $KZnF_3$:Li or $[100]_{010}$ waves, □ and ▽ (the two symbols represent two different measurements); for $[100]_{100}$ waves, 1057 ppm, ●; 725 ppm, ○; 1750 ppm, ◇, 1900 ppm, △.

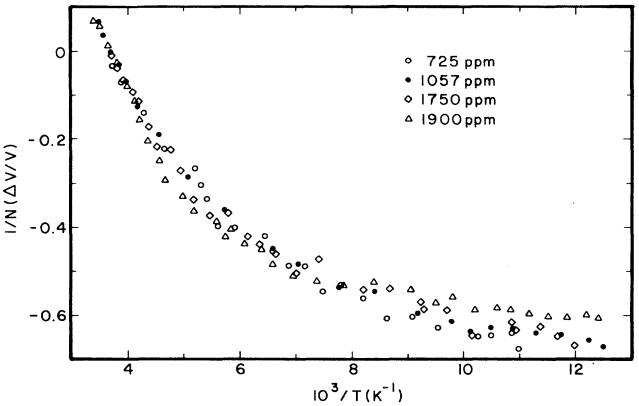


FIG. 6. Normalized $(1/N)\delta v/v$ vs $10^3/T$ in $KZnF_3$ for $[100]_{100}$ waves. The concentrations $N$ are those corresponding to the crystals mentioned in the caption of Fig. 5.

between the sound velocities in the pure and doped crystals. Due to the experimental uncertainty in the absolute velocities ($\sim 0.5\%$), these were arbitrarily assumed to be equal at 270 K. The relative velocity changes with temperature are in no way affected by this choice of "origin." The curves in Fig. 5 clearly indicate that, for [100] propagating waves, only the longitudinal ones are affected by the presence of lithium impurities. In this figure the three middle curves, in order of increasing $\delta v/v$, correspond, respectively, to the top half of the 1% crystal, the entire crystal, and the lower half of the same crystal. These results clearly reveal the presence of a strong concentration gradient in this crystal. They also indicate that the magnitude of the velocity change, $\delta v/v$, increases with impurity concentration in an approximately linear relationship. This can be seen in Fig. 6 where the same data have been normalized by an adjustable impurity concentration so as to superpose all curves onto the highest concentration one (1900 ppm). The concentrations obtained in this process are indicated on the figure and are found to be reasonably close to the concentration estimates obtained from flame absorption spectroscopy. Assuming a linear concentration gradient throughout the crystal, $c=-ax+b$, and using the above average concentrations, we find $a=965$ ppm/cm and $b=393$ ppm. Measurements of $\delta v/v$ for transverse waves propagating in the [110] direction (not shown), gave changes that were smaller than for [100] propagating waves, due primarily to the presence of residual strains along the growth axis of the crystals.

## VI. DISCUSSION

As indicated by the dielectric-loss measurements, the Li defect in $KZnF_3$ possesses an electric dipole. This requires that the Li impurity ion reside in a low symmetry position. The low activation energy measured for the defect relaxation however suggests that this position corresponds to only a shallow off-center potential well rather than a true interstitial one. Due to the monovalence of both K and Li, the Li impurity is most likely to substitute for K, in an off-center position. This is indeed the way in which Li resides in other potassium compounds such as KCl (Ref. 8) or $KTaO_3$ (Ref. 9). In the latter, in fact, the activation energy obtained for the lithium relaxation is exactly the same as the one we obtain in $KZnF_3$, 0.12 eV.

An estimate for the off-center distance can be obtained from the height of the loss peaks and using Eqs. (4) and (5). Given the location of the dielectric sample, just above the ultrasonic sample, and the concentration gradient observed in the latter, we estimate the average concentration in the dielectric sample to be approximately 300 ppm. The off-centering distance is then estimated at 0.15 Å. Due to the uncertainty in the concentration, however, this number should only be interpreted as an indication of the small off-centering distance of the lithium away from the lattice site.

In cubic crystals the dielectric tensor consists of a single coefficient. For this reason, dielectric measurements in these crystals can only provide limited information concerning the symmetry of a relaxing defect. In contrast, elastic measurements are more selective because the elasticity tensor consists of three independent coefficients,[10] $(C_{11}+2C_{12})$, $(C_{11}-C_{12})$ and $C_{44}$. The ultrasonic measurements in Figs. 5 and 6 reveal a change in the sound velocity of [100] longitudinal waves, which is proportional to the Li concentration. On the other hand, the velocity of [100] transverse waves is unaffected. The selection rules summarized in Table I then indicate that the only possible defect symmetry compatible with the ultrasonic results is either a tetragonal defect (off center in a ⟨100⟩ direction but symmetrical in the (100) plane) or a ⟨100⟩ orthorhombic defect [asymmetrical in the (100) plane, i.e., not an ellipsoid of revolution].

A more careful examination of the curves in Figs. 5 and 6 reveals two distinct temperature ranges. At high temperature, $\delta v/v$ appears to be proportional to $1/T$ with a relatively steep slope and, at lower temperature, it changes over to a much shallower slope. It is interesting to note that the same behavior has been observed for the $E_g$ mode in KCl, KBr, and KI doped with $CN^-$.[11] In those systems, it was shown that the strain ellipsoid associated with the $CN^-$ molecule was also not an ellipsoid of revolution, and possessed three distinct principal values, $\lambda_a, \lambda_b$, and $\lambda_c$. However, the authors did not seem to exploit this observation in order to explain the existence of two different temperature ranges in their $\delta v/v$ curves. In $KZnF_3$:Li, as well as in the above systems, we find a linear concentration dependence of $\delta v/v$ throughout both temperature ranges. This suggests that the crossover from one range to the other is not due to a change in the defect undergoing relaxation (e.g., pairs to single defect) but is rather due to a change in the relaxation process. We therefore propose that in $KZnF_3$:Li, as in KBr-KCN, the strain ellipsoid associated with the Li defect is not an ellipsoid of revolution, thereby allowing two distinct relaxation processes to be observed. This in fact is expected in the case of a ⟨100⟩ orthorhombic defect. As is indicated in Table I for such a defect, two distinct process-

es can contribute to the relaxation of $(C_{11}-C_{12})$ or $C_{11}$; the two corresponding relaxation times have been given in Eq. (8), and represent the two roots, $\tau_+$ and $\tau_-$, of a quadratic equation. In these two expressions, it is likely that the reorientation frequency $\nu_{12}$, between two equivalent positions of the impurity along one particular cube axis, will be much higher than all the other frequencies. Using this approximation, we see that $\tau_+^{-1}\simeq 2\nu_{12}$ and $\tau_-^{-1}\simeq 0$, corresponding, respectively, to a fast and a slow relaxation process, widely separated from each other. Similar cases of what is called "a frozen-free split" have been reported in the literature. In the light of this model, our results suggest that, at high temperature and $\nu_{12}$ being dominant, the Li impurity exhibits the character of an average defect of tetragonal symmetry. The slower relaxation that is then observed corresponds basically to a reorientation of the major axis of the strain ellipsoid and results in a steep $\delta v/v$ slope. From this slope and using Eq. (10), we find $\lambda_a-\lambda_{b,c}\simeq 0.013$, where $a,b$, and $c$ designate the major and minor axes of the ellipsoid and $\lambda_{b,c}$ can be taken as the average $(\lambda_b+\lambda_c)/2$. At lower temperature, the slower process becomes frozen, leaving only the fast relaxation active. As was indicated earlier, this fast process corresponds to a low-energy 90° rotation of the strain ellipsoid about its major axis. It therefore explains the observed shallower slope giving $(\lambda_b-\lambda_c)\simeq 0.006$. These values are smaller but of the same order of magnitude as other defects previously studied. We note, for example, that for lithium in KCl, the value of the ellipticity $\Delta\lambda$ is found to be larger, $\sim 0.05$, and with the lithium displaced $\sim 0.5$ Å ($2.5D$ electric dipole moment). In KBr, the ellipticity is comparable to that observed in $KZnF_3$ and corresponds to a smaller lithium displacement than in KCl.[11]

The only alternative explanation to the two-relaxation process model presented above would invoke Li-Li defect interactions at lower temperature. This explanation is not viable considering the linear concentration dependence throughout and the same cross-over temperature obtained for all concentrations.

We can now return to the case of $CN^-$ in KCl that an earlier study characterized as a ⟨110⟩ monoclinic defect and for which a sound wave of symmetry $E$ also revealed the existence of two distinct $\delta v/v$ slopes. Symmetry considerations presented earlier in Table I indicate that, for such a defect, it is the $T$ wave ($C_{44}$) and not the $E$ one ($C_{11}-C_{12}$) which should show two $\delta v/v$ slopes. On the other hand, if the $CN^-$ defect was ⟨100⟩ monoclinic, then two distinct processes would be possible and consequently two slopes should be observed. The authors of the previous study in fact concluded that "a ⟨110⟩ ellipsoid is the simplest model which can account for all the experimental results," nevertheless pointing out that the thermal conductivity results also agreed with the ⟨100⟩ Devonshire model. A ⟨100⟩ monoclinic symmetry, with a "frozen-free split" situation might well explain the apparent discrepancies between the various experimental results obtained on KCl:$CN^-$.

The dielectric-loss peak observed at 70 K for a 10-kHz frequency can be related to the ultrasonic $\delta v/v$ curves. Using the experimentally observed Arrhenius behavior of the relaxation time $\tau$, we would predict a loss peak at $10^3/T\simeq 6.7$ for a frequency of 45 MHz. On Fig. 6, this can be seen to correspond approximately to the crossover between the two temperature ranges. This observation could indicate that the Li jump which gives rise to the dielectic-loss peak corresponds to the slow process of reorientation of the strain ellipsoid major axis between cubic directions (tumbling motion). It is worth noting that one should not expect a dielectric peak due to a reorientation of the minor axes since, in the basal plane, the Li defect is only expected to possess an electric quadrupole.

Finally, the model proposed above requires a physical justification. This justification can be found in the existence of a soft mode in $KZnF_3$ which corresponds to a cog-wheel rotation of adjacent fluorine octahedra. Although the absence of a $C_{44}$ relaxation in this cubic system suggests that the major distortion associated with the defect has tetragonal symmetry, the lattice may well relax asymmetrically in the basal plane, due to the latent anharmonicity associated with the soft mode. The [001] off-center Li can then induce an asymmetrical relaxation of the lattice in the (001) plane due to a slight rotation of the nearby $F_6$ octahedra.

## VII. CONCLUSION

The effects of lithium relaxation on the velocity of ultrasonic waves and on the dielectric loss, lead us to conclude that lithium in $KZnF_3$ forms an off-center defect, most likely substituted for potassium. The existence, in the ultrasonic behavior, of a single linear concentration dependence but two distinct temperature ranges, suggest that two relaxation processes dominate, respectively, in these two ranges. By comparison with results obtained on KCl:$CN^-$, it is suggested that these are made possible by an asymmetry of the strain ellipsoid, itself due to the presence of a soft mode of tetragonal symmetry. The defect symmetry is then concluded to be ⟨100⟩ orthorhombic. At higher temperatures, the relaxation is dominated by the reorientation of the major axis of the ellipsoid and $\delta v/v$ exhibits a steeper slope due to $(\lambda_a-\lambda_b)\simeq 0.013$. At lower temperature, this major process becomes frozen or simply slows down, such that the relaxation is dominated by the fast reorientation of the minor axes of the ellipsoid. $\delta v/v$ then exhibits a shallower slope associated with a smaller ellipticity factor $(\lambda_b-\lambda_c)\simeq 0.006$.

## ACKNOWLEDGMENTS

This work was supported by a grant from the Department of Energy, DE.FG02.86 ER 45258. We would also like to thank Professor A. S. Nowick for very useful suggestions. The Laboratoire de Physique de l'Etat Condensé is Unité Associeé No. 807 du Centre National de la Recherche Scientifique.

[1]B. I. Halperin and C. M. Varma, Phys. Rev. B **14**, 4030 (1976); A. P. Levanyuk and A. S. Sigov, *Defects and Structural Phase Transitions* (Gordon and Breach, New York, 1988).
[2]P. A. Fleury and K. B. Lyons, in *Light Scattering near Phase Transitions,* edited by H. Z. Cummins and A. P. Levanyuk (North-Holland, Holland, 1983).
[3]N. Lehner *et al.*, J. Phys. C **15**, 6545 (1982).
[4]A. R. Von Hippel, *Dielectrics and Waves* (Wiley, New York, 1956).
[5]A. S. Nowick and B. S. Berry, *Anelastic Relaxation in Crystalline Solids* (Academic, New York, 1972).
[6]A. S. Nowick, Adv. Phys. **16**, 1 (1967).
[7]J. Toulouse and C. Launay, Rev. Sci. Instrum. **59**, 492 (1988).
[8]N. E. Byer and H. S. Sack, J. Phys. Chem. Solids, **29**, 677 (1968).
[9]U. T. Hochli, H. E. Weibel, and L. A. Boatner, Phys. Rev. Lett. **41**, 1410 (1978).
[10]J. F. Nye, *Physical Properties of Crystals* (Oxford University Press, London, 1957).
[11]N. E. Byer and H. S. Sack, Phys. Status Solidi **30**, 569 (1968); **30**, 579 (1968).